Decreasing Trend of Western North Pacific Tropical Cyclone Inner-Core Size over the Past Decades

Hanrui SHOU[1], Tim LI[1,2], Yuan SUN[3*], Lu WANG[1], and Jia LIU[1]

1 *Key Laboratory of Meteorological Disaster, Ministry of Education / Joint International Research Laboratory of Climate and Environmental Change, Nanjing University of Information Science & Technology, Nanjing* 210044, *China*
2 *International Pacific Research Center and Department of Atmospheric Sciences, University of Hawaii at Manoa, Honolulu, HI* 96822, *USA*
3 *College of Meteorology and Oceanography, National University of Defense Technology, Nanjing* 211101, *China*

(Received December 15, 2020; in final form April 15, 2021)

ABSTRACT

Studies on tropical cyclone (TC) inner-core size have become increasingly active in recent years. However, few studies have investigated the trend of TC inner-core size. Here, we introduce a new index to measure TC inner-core size and calculate the observed trend. This index can greatly reduce the influence of data heterogeneity and uncertainty. It also considers public concern because the new index is mainly determined by the inner-core size of strong TCs, which attract more public attention than weak TCs. The results show that in the past decades, TC inner-core size has a significant downtrend that is significant above the 99% confidence level when the new index is used. We also show that this trend is probably related to the increase in TC intensity and relatively small inner-core size of strong TCs. Moreover, relative sea surface temperature (SST) is assumed to make contributions to the downtrend of TC inner-core size, which has a significant negative correlation with the new index.

Key words: tropical cyclone (TC), inner-core size, trend, intensity

Citation: Shou, H. R., T. Li, Y. Sun, et al., 2021: Decreasing trend of western North Pacific tropical cyclone inner-core size over the past decades. *J. Meteor. Res.*, **35**(4), 635–645, doi: 10.1007/s13351-021-0214-z.

1. Introduction

Due to the importance of intensity, frequency, and track in tropical cyclone (TC) forecasting (Emanuel, 1999), the trends of these characteristic features of TCs are a hot research topic (Chan and Kepert, 2010; Zhao et al., 2018). However, the potential destructive power of TC, which is of great public concern, is not only related to the above-mentioned features (e.g., TC intensity, frequency, and track; Carrasco et al., 2014; Wu and Lei, 2014; Xu and Wang, 2015; Wang and Toumi, 2018), but also related to TC size. Compared with a TC with a small size, a TC with a large horizontal extent of damaging winds can impact a much larger area, even if the intensities of the two TCs are similar (Chan and Chan, 2012, 2013, 2014, 2018). Therefore, it is critical to study the trend of TC size under global warming.

There are many different approaches to determine TC size. For example, the radius of maximum wind (RMW), the radius of the TC eye, the gale-force wind [34 knots (kt)], and the radius of outermost-enclosed isobar (ROCI) can all be used to determine TC size (Merrill, 1984; Weatherford and Gray, 1988a; Kimball and Mulekar, 2004; Knaff et al., 2007; Moyer et al., 2007; Maclay et al., 2008; Matyas, 2010). Among the factors mentioned above, the most representative one of TC inner-core size is the RMW (Chan and Chan, 2018). On the one hand, the RMW can be roughly taken as the radius of TC eyewall, where the destructive power is the largest and thus is of public concern. On the other hand, the RMW is determined based on relative values of TC wind measurements rather than the absolute values, and thus is expected to be relatively less uncertain (Quiring et al., 2011).

The RMW pertains to TC inner-core size. In 1988, Weatherford and Gray (1988b) defined the "inner core" and "outer core" of a TC, and found that changes in the

Supported by the National Natural Science Foundation of China (42075035 and 41605072).

*Corresponding author: sunyuan1214@126.com

inner-core strength and outer-core strength often occur independently of each other. Relatively few studies investigated the causes for TC inner-core changes. Hill and Lackmann (2009) found that the intensity and coverage of precipitation occurring outside the TC core are highly sensitive to environmental humidity, which can affect the inner-core size based on idealized numerical simulations. Xu and Wang (2010a) found that the TC inner-core size is largely determined by the size of the initial vortex. Their follow-up work indicated that the ocean–atmosphere entropy fluxes are crucial for the growth of storm's inner-core size (Xu and Wang, 2010b). The above-mentioned studies mainly focused on analyzing single TC inner-core size, whereas little was done to explore long-term climatic trend of TC inner-core size. Grinsted et al. (2012) showed that the frequency of large surge events (roughly corresponding to TC size) has a statistically significant trend from 1923 to 2012. However, they did not directly address the trend of TC size.

Our overall goal of this study is to examine the trend of TC inner-core size in the past decades, and explore the possible causes for the trend. We focus on the western North Pacific (WNP) TCs with TC size information extracted from the China Meteorological Administration (CMA) dataset (1981–2016) and Japan Meteorological Agency (JMA) dataset (1977–2016). During this study period of 1981–2016, due to the existence of geostationary satellites, the accuracy of TC data was greatly improved compared to that in the pre-satellite era (before 1965) (Kossin, 2019; Moon et al., 2019). In addition, on the basis of our previous studies, we focus on the potential destructive effects of TCs when studying the trend of TC inner-core size, that is, we use a new approach to characterize TC inner-core size. By using the power dissipation index (PDI) as the weighting coefficient, the RMW is calculated and used to evaluate the trend of TC size. As indicated in Sun et al. (2018), this method can greatly reduce the uncertainty caused by data heterogeneity. Meanwhile, we take public concern into consideration since the inner-core size is mainly determined by strong TCs; such TCs attract more public attention compared to weak TCs.

2. Data and methods

We mainly use the latest dataset for size analysis provided by the CMA (Lu et al., 2017), which is available at https://tcdata.typhoon.org.cn/tcsize.html. The dataset that contains the TC size information was first released in 2017. All TCs captured by satellites in the WNP are included in this dataset, which covers the area 0°–60°N, 100°E–180°, including the South China Sea. The TC location, intensity, and 34-kt wind radius at 6-h interval for the period 1981–2016 are included in this dataset. The JMA best track data (available at https://www.jma.go.jp/jma/jma-eng/jma-center/rsmc-hp-pub-eg/trackarchives.html) that cover the period 1977–2016 are also used in the present study. The JMA data include maximum wind speed and TC radii corresponding to 30- and 50-kt wind speeds, respectively. Only those TCs over the WNP with maximum wind speed larger than 34 kt are selected for the present study. In total, the same 819 TCs are selected from each dataset. We use the model from Chavas et al. (2015) for the complete radial structure to calculate the TC RMW. The model is constructed by mathematically merging existing theoretical solutions for the radial wind structure at the top of the boundary layer in the inner ascending and outer descending regions. In the present study, the model is expressed by:

$$M_{\max}\frac{2}{(r_a/\mathrm{RMW})^2+1}=M_a, \tag{1}$$

$$M_a=r_aV_a+\frac{1}{2}fr_a^2, \tag{2}$$

$$M_{\max}=\mathrm{RMW}\cdot V_{\max}+\frac{1}{2}f\cdot\mathrm{RMW}^2, \tag{3}$$

where M_a is the absolute angular momentum at TC radius of a from the axis of rotation, and V_a is the azimuthal velocity at TC radius of a; same as M_a and V_a, $M_{\max}$ and $V_{\max}$ are the absolute angular momentum and azimuthal velocity at the RMW of the TC; f is the Coriolis parameter. Using the size information of the 34-kt wind radius (r_{34}) in the CMA data and the TC wind radius, e.g., r_{30} (r_{50}), corresponding to the wind speed of 30 kt (50 kt) in the JMA data into the above algorithms, we can derive the TC wind profile model and eventually obtain the TC RMW. For the JMA dataset, if r_{30} and r_{50} are both available for a specific TC, the results obtained by using r_{50} in the algorithms are taken as the final results. This is because r_{50} is closer to RMW, and thus the biases are expected to be smaller.

We first use the averaged RMW as the indicator of TC inner-core size. The RMW used here is not weighted based on TC strength, that is, the weighting factors are the same no matter whether the TC is strong or weak. We term it $\mathrm{RMW_{AVE}}$. The algorithms are expressed as follows.

For the $\mathrm{RMW_{AVE}}$ of a single TC:

$$\mathrm{RMW_{AVE}}=\frac{\int_0^\tau \mathrm{RMW}(t)\mathrm{d}t}{\tau}; \tag{4}$$

for the annual mean $\mathrm{RMW_{AVE}}$ of all TCs:

$$\mathrm{RMW}_{\mathrm{AVE\text{-}annual}}=\frac{\sum_{j=1}^{N}\mathrm{RMW}_{\mathrm{AVE}}(j)}{N}, \quad (5)$$

where τ is the lifetime of a TC, RMW(t) is the RMW at a specific time, N is the total number of TCs in a specific year, j is the sequential number of a specific TC, and $\mathrm{RMW}_{\mathrm{AVE}}(j)$ is the $\mathrm{RMW}_{\mathrm{AVE}}$ of the jth TC.

The PDI is the index that can estimate the potential destructive power of TC. It is an index related to TC duration, frequency, and intensity (Emanuel, 2005; Camargo et al., 2007). The PDI is calculated by:

$$\mathrm{PDI}=\int_0^{\tau} V_{\max}^3(t)\mathrm{d}t. \quad (6)$$

The RMW calculated by using the TC PDI as the weighting factor is termed as $\mathrm{RMW}_{\mathrm{PDI}}$.

For the $\mathrm{RMW}_{\mathrm{PDI}}$ of a single TC:

$$\mathrm{RMW}_{\mathrm{PDI}}=\frac{\int_0^{\tau}\mathrm{RMW}(t)\cdot V_{\max}^3(t)\mathrm{d}t}{\int_0^{\tau} V_{\max}^3(t)\mathrm{d}t}. \quad (7)$$

For annual mean $\mathrm{RMW}_{\mathrm{PDI}}$:

$$\mathrm{RMW}_{\mathrm{PDI\text{-}annual}}=\frac{\sum_{j=1}^{N}\mathrm{RMW}_{\mathrm{PDI}}(j)\cdot V_{\max}^3(j)}{\sum_{j=1}^{N} V_{\max}^3(j)}. \quad (8)$$

Monthly mean sea surface temperature (SST) data with 2° × 2° horizontal resolution are from the NOAA Extended Reconstructed SST version 4 of the US (Smith and Reynolds, 2003).

3. Results

3.1 *Trend of TC RMW over the WNP in the past 40 years*

We first used $\mathrm{RMW}_{\mathrm{AVE}}$ to calculate the inner-core size. Although $\mathrm{RMW}_{\mathrm{AVE}}$ can reflect the TC RMW trend to a certain extent, it contains some uncertainty. On the one hand, the TC intensity is small at the times of genesis and extinction, which makes it hard to observe TCs at these times. Meanwhile, there exist large differences in TC genesis and extinction between different observational datasets, which leads to large biases of observations at the times of TC genesis and extinction (Kruk et al., 2010; Sun et al., 2018). As a result, large biases are found in $\mathrm{RMW}_{\mathrm{AVE}}$ averaged over the TC lifetime. On the other hand, public attention is focused on strong TCs (Kossin et al., 2016). Based on the above discussion, we define a new TC size index, i.e., the RMW weighted by TC PDI ($\mathrm{RMW}_{\mathrm{PDI}}$), which is then used to represent TC inner-core size and assess TC inner-core size trend.

Compared with $\mathrm{RMW}_{\mathrm{AVE}}$, the impact of data uncertainty on $\mathrm{RMW}_{\mathrm{PDI}}$ is greatly reduced. This is due to several factors. (1) $\mathrm{RMW}_{\mathrm{PDI}}$ is not sensitive to the relatively inaccurate data during the TC lifetime. The variable $V_{\max}^3$ is used as the weighting factor for the calculation of $\mathrm{RMW}_{\mathrm{PDI}}$. It is quite small at the time when the TC is weak (e.g., TC genesis and extinction), namely, $\mathrm{RMW}_{\mathrm{PDI}}$ at the time of TC genesis or TC extinction only has low weight. Moreover, measuring $V_{\max}^3$ at these times is more difficult and less accurate (Moon et al., 2019). As a result, $\mathrm{RMW}_{\mathrm{PDI}}$ is more accurate than $\mathrm{RMW}_{\mathrm{AVE}}$ due to its insensitivity to relatively inaccurate data, which makes $\mathrm{RMW}_{\mathrm{PDI}}$ insensitive to data observed at the time of TC genesis or TC extinction. (2) $\mathrm{RMW}_{\mathrm{PDI}}$ is not sensitive to weak TCs. Weak TCs tend to have a larger area of weak wind (e.g., the radius of 34-kt wind) than strong wind, which means that they are much more difficult to be observed accurately. Therefore, observations of strong TCs are generally more reliable than those of weak TCs. Since strong TCs with larger PDI have greater weight in the calculation of $\mathrm{RMW}_{\mathrm{PDI}}$, the uncertainty caused by observations of weak TCs with smaller PDI has weak impact on the reliability of $\mathrm{RMW}_{\mathrm{PDI}}$. (3) More consistent results of $\mathrm{RMW}_{\mathrm{PDI}}$ can be obtained by using datasets from different agencies. Large differences are frequently found between datasets from different agencies (Sun et al., 2018), and the differences are especially large in observations of weak TCs. The characteristics of $\mathrm{RMW}_{\mathrm{PDI}}$ discussed above can greatly reduce the impact of these differences on the calculation of $\mathrm{RMW}_{\mathrm{PDI}}$: the mean difference is 0.38 km yr^{-1} for $\mathrm{RMW}_{\mathrm{PDI}}$ and 0.72 km yr^{-1} for $\mathrm{RMW}_{\mathrm{AVE}}$ (Fig. 1).

Figure 2 displays the 36-yr (1981–2016) annual mean RMW of TCs calculated from the latest CMA dataset that includes TC size information. The annual mean TC $\mathrm{RMW}_{\mathrm{AVE}}$ is presented in Fig. 2a, which shows that the $\mathrm{RMW}_{\mathrm{AVE}}$ trend is -4.2 ± 2.4 km decade^{-1} during the past 36 years. Note that this trend is statistically significant at the 99% confidence level, indicating that there exists a distinct downward trend for $\mathrm{RMW}_{\mathrm{AVE}}$. $\mathrm{RMW}_{\mathrm{PDI}}$ demonstrates a trend of -2.3 ± 1.2 km decade^{-1} (Fig. 2b), which is statistically significant at the 99% confidence level, suggesting that $\mathrm{RMW}_{\mathrm{PDI}}$ also declines distinctly.

The results from the JMA data are presented in Fig. 3. The trend of $\mathrm{RMW}_{\mathrm{AVE}}$ (5.5 ± 4.8 km decade^{-1}) is statistically significant at the 99% confidence level, which is different to the result obtained from the CMA dataset. The $\mathrm{RMW}_{\mathrm{PDI}}$ from the JMA data is similar to that from the CMA data; both show a significant declining trend. The trend of $\mathrm{RMW}_{\mathrm{PDI}}$ from the JMA data is -3.3 ± 2.9 km decade^{-1}, which is statistically significant at the 99% confidence level.

The results of $\mathrm{RMW}_{\mathrm{AVE}}$ calculated from the CMA and JMA data are quite different. When using $\mathrm{RMW}_{\mathrm{PDI}}$, however, the difference is greatly reduced and the trends

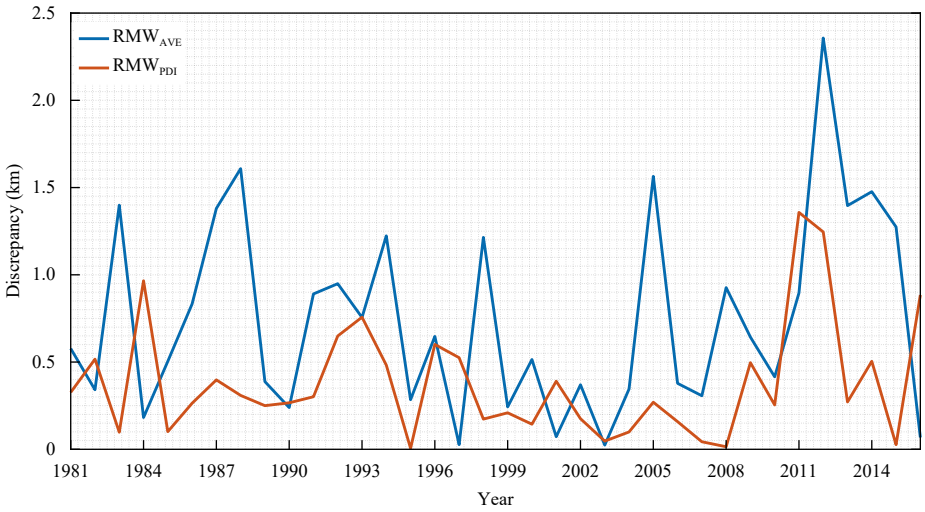

Fig. 1. Discrepancies of standardized RMW_{AVE} (RMW_{PDI}) by using JMA and CMA datasets. JMA and CMA data used to obtain RMW_{AVE} and RMW_{PDI} are standardized before calculation as RMW_{AVE} and RMW_{PDI} have substantially different mean values and variance.

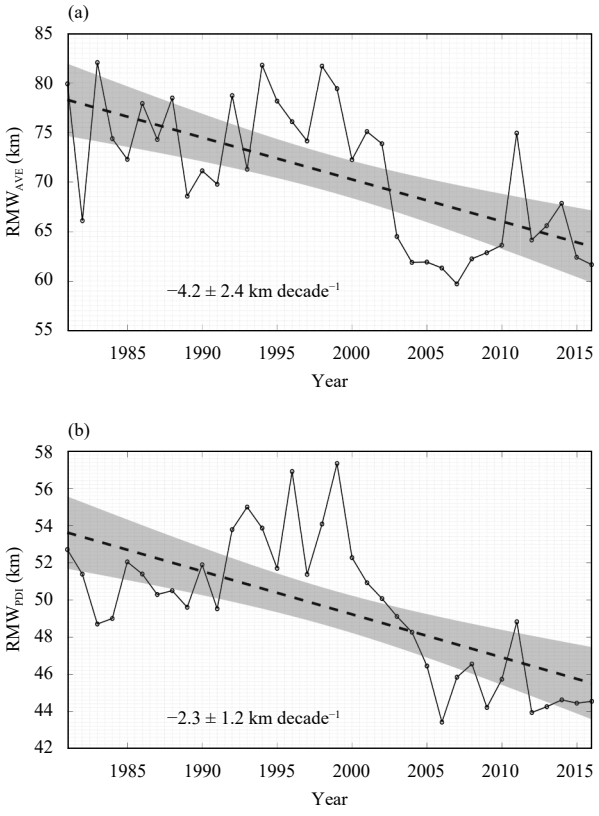

Fig. 2. The radius of maximum wind (RMW) of the western North Pacific (WNP) tropical cyclones (TCs) during 1981–2016 based on the CMA data. (a) Time series of annual mean RMW and (b) RMW weighted by TC destructive potential index over the WNP calculated from the CMA data. Linear trend (dashed line) is shown with the 95% two-sided confidence intervals (shading).

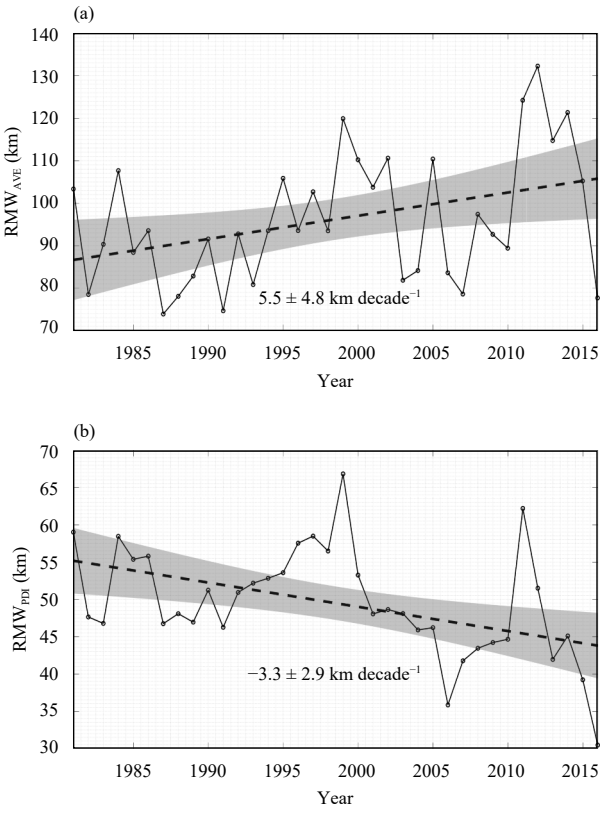

Fig. 3. As in Fig. 2, but for using the JMA data.

of RMW_{PDI} calculated from the two datasets are consistent. This is attributed to the fact that RMW_{PDI} is calculated by using the TC PDI as a weighting factor, which greatly reduces the impact of data uncertainty on RMW.

Data uncertainty usually has a great impact on the robustness of the RMW obtained. The RMW_{AVE} trend is severely affected by data heterogeneity. As stated by Kruk et al. (2010), compared with the period of strong intensity in a TC's lifetime, it is harder to collect observations during the period of weak intensity in a TC's lifetime; and large uncertainties are found in these observa-

tions. The data of weak TC intensity account for a large percentage of the best-track data, which makes RMW_{AVE} easily affected by the RMW when TC intensity is weak and large uncertainties exist in RMW_{AVE}. In contrast, RMW_{PDI} is largely determined by RMW when TC intensity is strong, which avoids the uncertainty associated with weak TCs. Therefore, we can reach the conclusion that the observed TC RMW, especially strong TC RMW, shows a significant declining trend in the study period.

3.2 *Mechanisms for the downtrend of TC RMW over the WNP*

To study the cause for the rapid decline of TC RMW_{PDI}, we first examine TC intensity. This is because several studies have pointed out that TC intensity is correlated with TC RMW. For example, Carrasco et al. (2014) found that at different stages of TC development, TC RMW is negatively correlated with TC intensity change at various degrees. Similarly, Stern et al. (2015) indicated that in idealized numerical experiments, the reduction of TC RMW happens simultaneously with TC intensification. In the present study, we use V_{AVE} and PDI to depict TC intensity, with V_{AVE} being the averaged wind speed over the TC lifetime. Averages of RMW_{AVE}, RMW_{PDI}, V_{AVE}, and PDI for these TCs during their lifetimes are calculated. The results based on the CMA data are displayed in Fig. 4, which shows that RMW_{AVE} is significantly negatively correlated with V_{AVE}, and that RMW_{PDI} is significantly negatively correlated with the PDI. For the convenience of displaying results, ln(PDI) is used in Fig. 4b. The correlation coefficient between RMW_{AVE} and V_{AVE} is −0.68, and the correlation coefficient between RMW_{PDI} and PDI is −0.54. Both are above the 99% confidence level. The fitting curve also passes the significance test at the 99% confidence level, and both test values p are less than 0.001, suggesting that the fitting curve can well describe the linear relationship between TC intensity and TC size. The results from the JMA data are shown in Fig. 5. Based on the above results, we speculate that the decrease in TC RMW_{PDI} in the past few decades may be related to the increase in TC intensity.

Considering the fact that RMW_{PDI} is weighted by the PDI, it is obvious that stronger TCs with larger PDI would have greater impacts on the calculated RMW_{PDI} trend. Therefore, based on the value of the PDI, we define the TCs that rank in the top 30% each year as strong TCs. Figure 6 shows that the annual mean value of the PDI for strong TCs has a significant upward trend, which is above the 95% confidence level. It is well known that TC intensification is often accompanied by a contraction in RMW (Schubert and Hack, 1982; Hack and Schubert, 1986), which means that when TCs reach

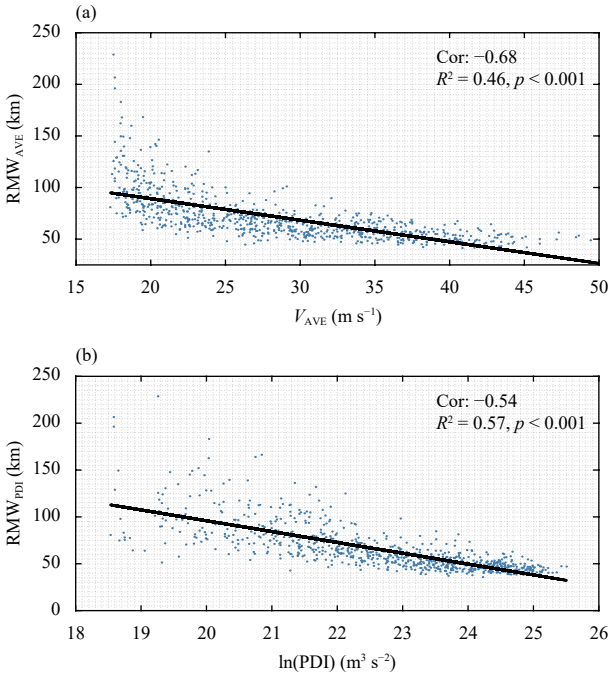

Fig. 4. Scatterplots of TC RMW and TC intensity based on the CMA data: (a) between RMW_{AVE} and V_{AVE}, and (b) between RMW_{PDI} and PDI. For the convenience of displaying results, ln(PDI) is used in (b). The black lines are regression curves, and both pass significance test at the 99% confidence level. Correlation coefficient (Cor), the coefficient of determination (R^2), and p value are also given.

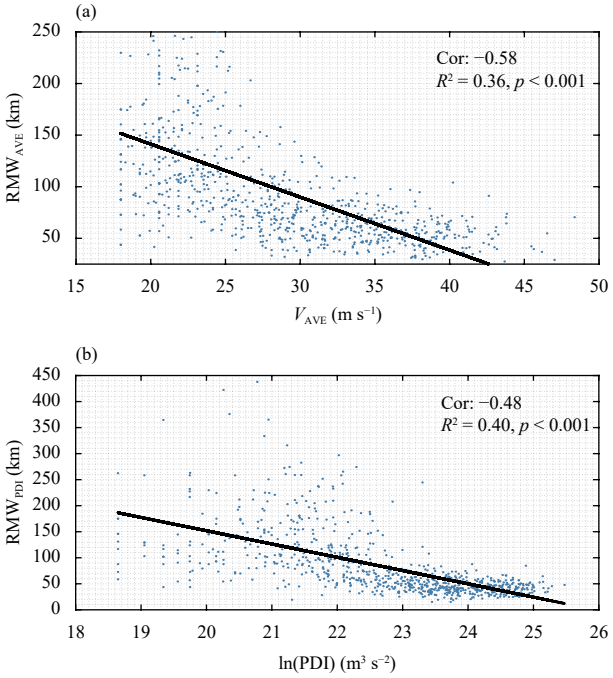

Fig. 5. As in Fig. 4, but for using the JMA data.

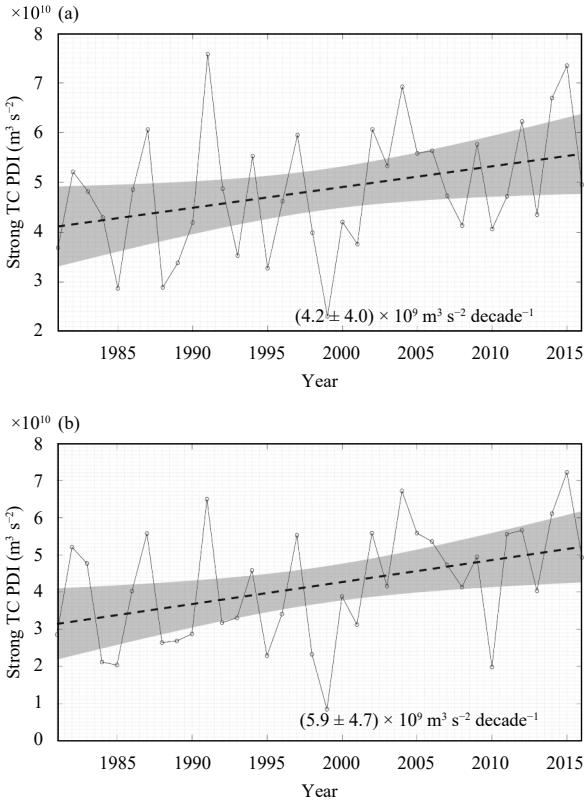

Fig. 6. Strong TC PDI over the WNP of (a) the CMA data and (b) the JMA data. Both are above the 95% confidence level. Based on the value of the PDI, the TCs that rank in the top 30% each year are defined as strong TCs.

their maximum intensity, their RMW would shrink in those moments. The moments with small RMW would have a great weight on RMW_{PDI} as mentioned. As strong TCs intensity has a significant upward trend in the past decades, with the significant inverse correlation coefficient between intensity and RMW_{PDI}, RMW_{PDI} would have a downward trend as a result.

What is the cause for the PDI of strong TCs rising each year? As suggested by Webster et al. (2005), increasing TC frequency and intensity might be related to increasing SST. Based on this, we hypothesize that changes in the intensity of strong TCs might be related to changes in the WNP SST. To verify this hypothesis, we define the WNP (5°–25°N, 120°E–180°) as the major area of TC activities. Since we focus on the main TC season (July to November, or JASON; Kossin et al., 2016), SST is averaged over July–November in this study. The results indicate that in the past 40 years, the WNP SST demonstrates a significant upward trend. Meanwhile, 5-yr moving averages of annual mean PDI of strong TCs and the WNP SST are calculated to filter out high frequency interannual disturbances. The results show that annual mean WNP SST and annual mean PDI of strong TCs are well correlated. Based on the CMA data, the correlation coefficient between the WNP SST and annual mean PDI of strong TCs is 0.44, which is significant at the 99% confidence level. The correlation coefficient is 0.40 based on the JMA data and above the 99% confidence level (figure omitted). The above results imply that the increasing SST has greatly affected the PDI of strong TCs over the WNP. Meanwhile, we find that the WNP SST is well correlated with RMW_{PDI} (Fig. 7); the correlation coefficient between them is −0.51 based on the CMA data and −0.34 based on the JMA data, and both are significant at the 95% confidence level. Therefore, the increase of SST is expected to have a significant impact on the PDI and RMW_{PDI} of strong TCs under the global warming.

According to published studies, relative SST also has a significant impact on TC activities (Sun et al., 2013). Relative SST means TCs' environmental SST relative to the tropical mean SST. In our study, the tropical mean SST is defined by using the area over 5°–25°N, 120°E–180°. As suggested by Vecchi and Soden (2007), the high relative SST favors the development of TC intensity. This may contribute to smaller RMW due to the aforementioned inverse relationship between intensity and RMW of strong TCs. Therefore, we calculated the averaged relative SST_{PDI} (similar to the RMW_{PDI} calculation method) within different radii from the TC center, through all the 819 TC samples from the JMA data. The result shows that the relative SST_{PDI} has a significant negative correlation with RMW_{PDI} (Fig. 8). This indicates that the decrease of RMW_{PDI} is closely related to the rise of relative SST_{PDI}.

According to previous studies, the physical basis for relationship among relative SST, TC intensity, and inner-core size may be related to the air–sea interface and convective activity. The air–sea interface plays an important role on TC intensity change caused by relative SST. As the inflow air gets closer to the eyewall, the colder remote SST from the TC center (which can lead to the result that the TC would have warmer relative SST) can gradually decrease the surface air temperature and moisture near the TC center, and thus increase air–sea temperature differences and moisture differences between the TC center and the area outside it, which will lead to more energy fluxes entering the eyewall and increasing the TC intensity (Sun et al., 2013). Moreover, convective activity and inertial stability contribute to the anticorrelation between TC intensity and TC inner-core size. TCs with large RMW need more convective heating during intensification (Wu and Ruan, 2021) and have better inertial stability, which inhibits inflow from transporting higher

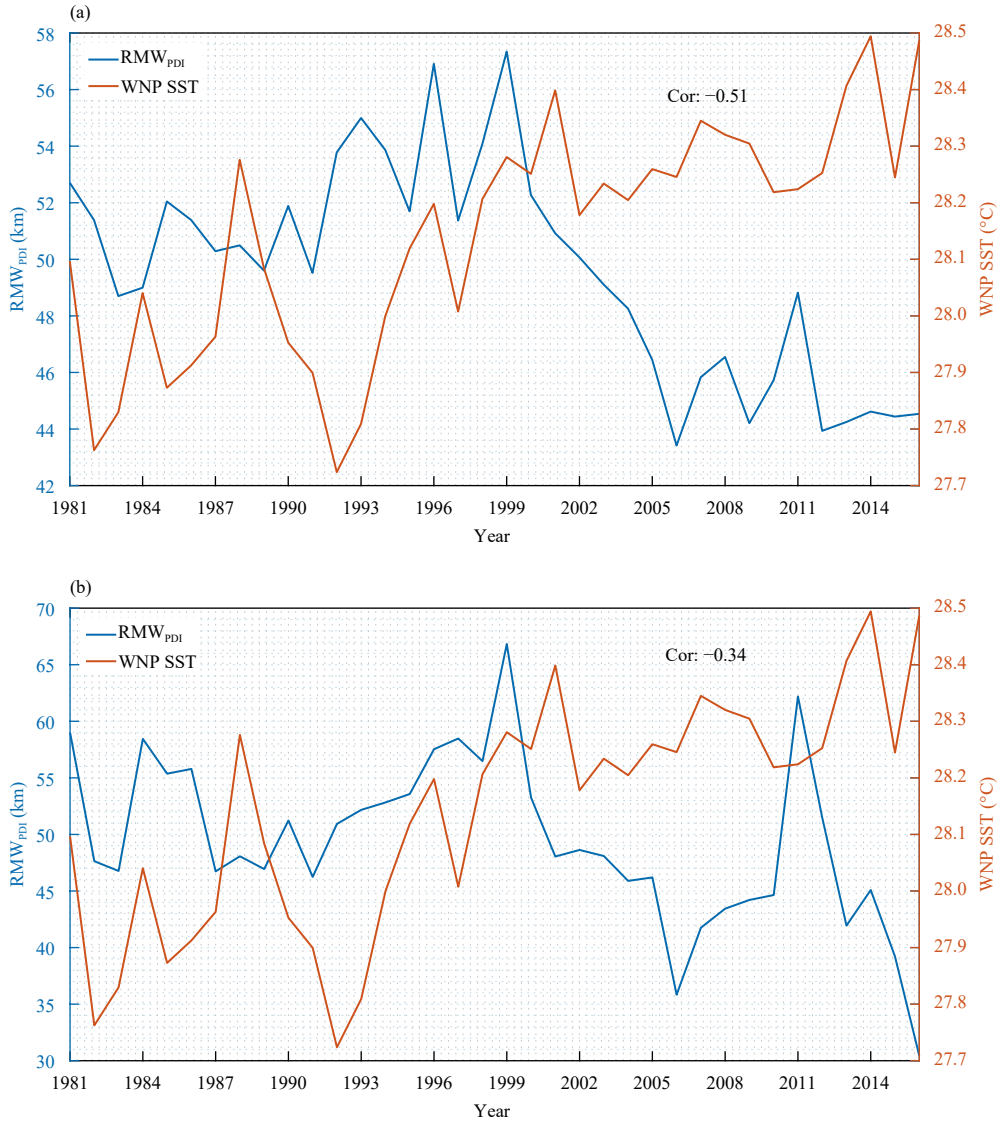

Fig. 7. WNP SST and RMW_{PDI} over the WNP by using (a) the CMA data and (b) the JMA data. The WNP is defined as the area of 5°–25°N, 120°E–180°, which is the main area of TC activities. Correlation coefficients are also given.

angular momentum air inward within the boundary layer (Carrasco et al., 2014); this causes TCs with large RMW to have more difficulties to reach their potential maximum intensity and they are more likely to be weaker than TCs with smaller RMW.

4. Summary and discussion

The new index RMW_{PDI} proposed in the present study has high assessment accuracy and can be derived from a wide range of datasets. It also considers public concern. Using this index calculated from the CMA and JMA datasets, the TC size trend over the WNP in the past decades is revisited. The results indicate that compared with RMW_{AVE}, RMW_{PDI} has less uncertainty and demonstrates a significant downward trend. The study of a large number of TC samples shows that the TC RMW is significantly negatively correlated with TC intensity. Furthermore, strong TCs are selected from the TC samples based on the PDI. It is found that the annual mean PDI for strong TCs demonstrates a significant upward trend, which is attributed to the distinct increase in SST of the WNP. As a result, the enhancement of TC PDI further contributes to the decrease of RMW. Relative SST also contributes to the decrease through the air–sea interface.

We also note that there is a significant, abrupt decadal change of RMW_{PDI} around 1999 (Fig. 9). Since RMW_{PDI} has a significant positive correlation with the latitude calculated by using the PDI as the weighting factor, which is termed as LAT_{PDI} (similar to the RMW_{PDI} calculation method; the correlation coefficient is 0.43 from the CMA

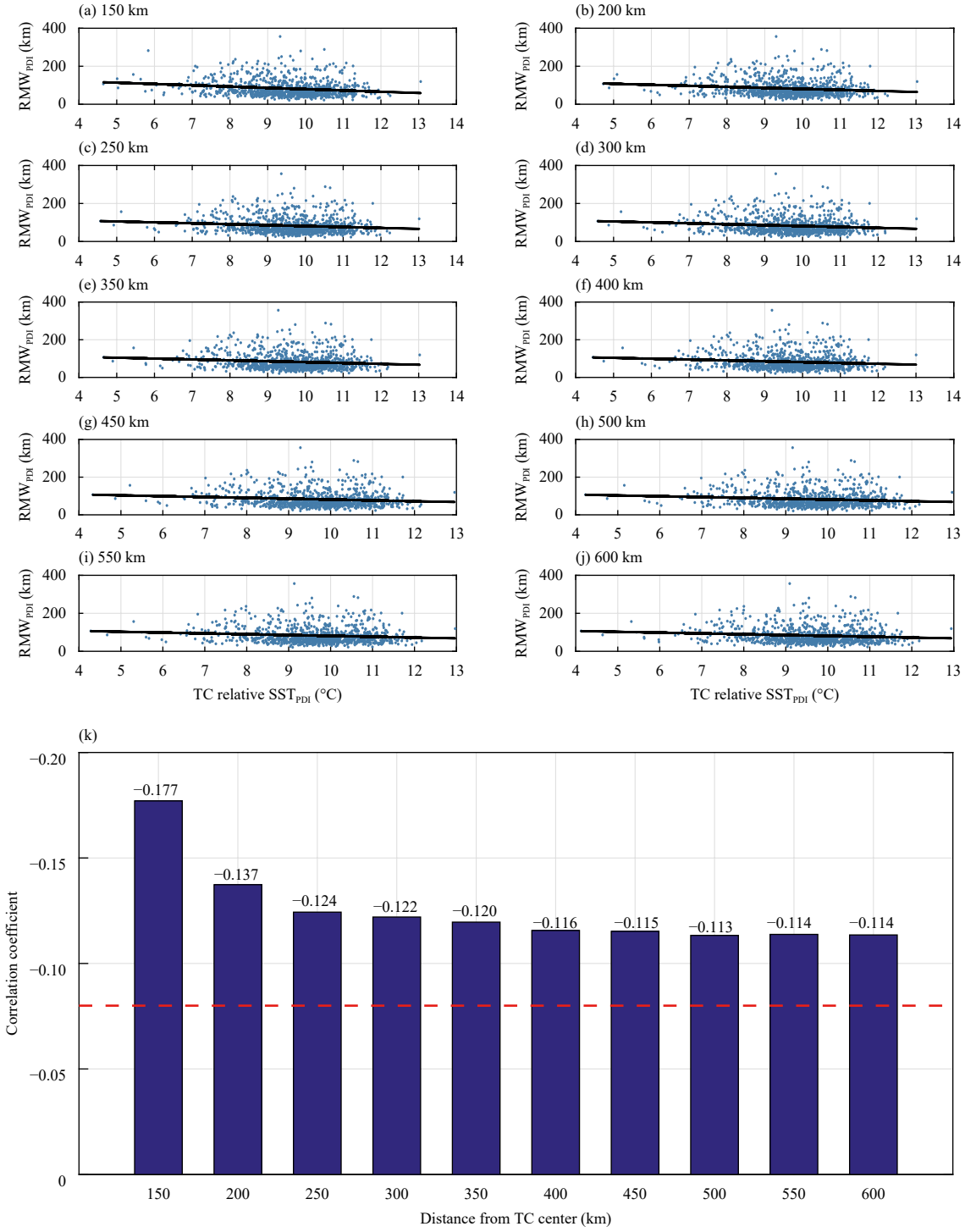

Fig. 8. Correlation between RMW_{PDI} and relative SST_{PDI} within different radius from the TC center. (a–j) The scatter plots within radii of 150–600 km. The black lines are regression curves. (k) The correlation coefficient, with the red dashed line indicating the 99% confidence level.

dataset and 0.42 from the JMA), and as Sun et al. (2018) showed that the trend of WNP TC migration reversed during the recent warming slow-down period (after 1999), it is assumed that the change of TC latitude may contribute greatly to the abrupt decadal change of RMW_{PDI}. From Sun et al. (2018), LAT_{PDI} first had an upward trend, and then after 1999 had a downward trend, which is consistent with the trend of RMW_{PDI} in this study; and the change of LAT_{PDI} is mostly contributed by SST. These results imply that in the background of global warming and tropical expansion (Kossin et al., 2014), TCs had a migration to the equator in the average latit-

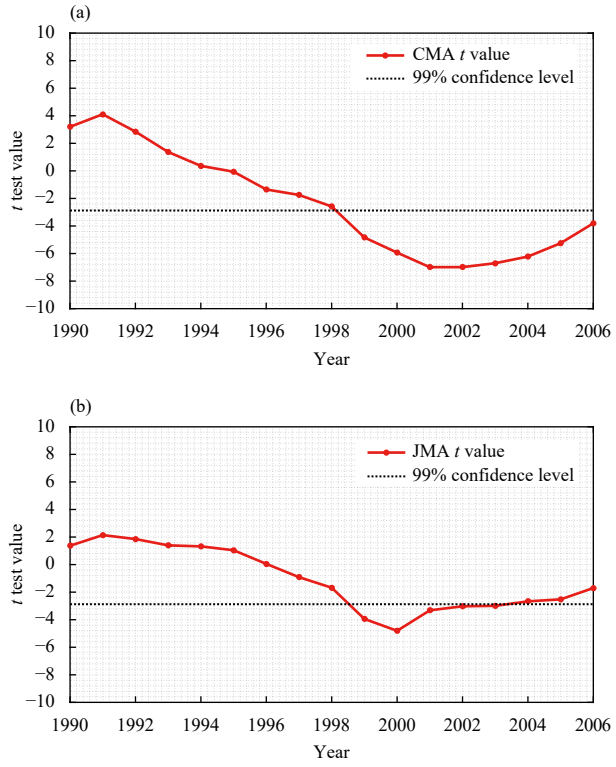

Fig. 9. Abrupt decadal change of RMW_{PDI}. Moving t test for the RMW_{PDI} based on (a) the CMA data and (b) the JMA data. The black dotted line indicates the 99% confidence level.

ude where TCs have achieved their lifetime maximum intensity after 1999, and it led to the decrease of RMW_{PDI}. However, detailed mechanism still needs to be studied.

Note that despite the upward trend of TC PDI caused by SST increase, it is still far to reach a robust conclusion that the downward trend of TC RMW is caused by the global warming. This is because, as Webster et al. (2005) argued, the data only cover 36-yr period, which is not long enough to justify the relation between global warming and TC RMW change. Meanwhile, it is well known that interannual changes in TC activity are to a great extent affected by natural variabilities like El Niño–Southern Oscillation (ENSO), Pacific decadal oscillation (PDO), and interdecadal Pacific oscillation (IPO). To explore the impacts of natural variabilities on TC RMW_{PDI}, the time series of annual mean TC RMW is regressed onto Niño-3.4, PDO, and IPO indexes (Henley et al., 2015), termed as $\varepsilon_{Niño\text{-}3.4}$, ε_{PDO}, and ε_{IPO}, respectively. Each ENSO, PDO, and IPO variability was removed from the time series of annual mean RMW_{PDI} by regressing RMW_{PDI} onto the annual mean index value and forming time series of the residual of the regression. The coefficient of determination R^2 and p value are given in Table 1. Detailed methods can be found in Kossin et al. (2014). The monthly mean Niño-3.4, PDO, and IPO

Table 1. Linear trends of annual mean RMW_{PDI} and their regression residuals (km decade^{-1}) for the CMA and JMA datasets

	CMA data	JMA data
RMW_{PDI}	−2.3 ± 1.2	−3.3 ± 2.9
$\varepsilon_{Niño\text{-}3.4}$	−2.2 ± 0.95	−3.2 ± 2.1
R^2, p value	0.42, < 0.001	0.22, 0.004
ε_{PDO}	−2.2 ± 0.98	−3.6 ± 2.1
R^2, p value	0.41, < 0.001	0.25, 0.002
ε_{IPO}	−2.3 ± 0.96	−3.5 ± 2.1
R^2, p value	0.39, < 0.001	0.27, 0.001

indexes are from NOAA's Earth System Research Laboratory Physical Sciences Division (Mantua et al., 1997; Rayner et al., 2003). Similar to SST, the Niño-3.4, PDO, and IPO indexes are also averaged over July–November. The results indicate that RMW_{PDI} still shows a significant downward trend, suggesting that natural variabilities like ENSO, PDO, and IPO have no strong impacts on TC RMW_{PDI}. Therefore, compared with the theory based on the known dominant modes of variability (Murakami et al., 2012; Kossin et al., 2014, 2016), the mechanism associated with the regional pattern of SST change is a more convincing explanation for the downward trend of the TC inner-core size over the WNP. This implies but does not necessarily mean that the natural variabilities did not contribute significantly to the downward trend as expected, since it is difficult to distinguish the contributions of relative SST variability and natural variabilities based on the short time series.

For the future work, we plan to investigate the cause for the large differences in RMW between TCs with the same intensity, as shown in Fig. 2a. Our preliminary hypothesis is that the differences in environmental background at the initial stage of TC genesis eventually lead to differences in TC RMW. This will be addressed in our further publication.

Acknowledgments. Thanks to Zanmin Xu for her help. We thank the CMA and JMA for providing the TC data, and NOAA for providing interpolated monthly SST data.

REFERENCES

Camargo, S. J., K. A. Emanuel, and A. H. Sobel, 2007: Use of a genesis potential index to diagnose ENSO effects on tropical cyclone genesis. *J. Climate*, **20**, 4819–4834, doi: 10.1175/JCLI4282.1.

Carrasco, C. A., C. W. Landsea, and Y.-L. Lin, 2014: The influence of tropical cyclone size on its intensification. *Wea. Forecasting*, **29**, 582–590, doi: 10.1175/WAF-D-13-00092.1.

Chan, J. C. L., and J. D. Kepert, 2010: *Global Perspectives on Tropical Cyclones*: *From Science to Mitigation*. World Scientific Publishing, Singapore, 325–360, doi: 10.1142/7597.

Chan, K. T. F., and J. C. L. Chan, 2012: Size and strength of tropical cyclones as inferred from QuikSCAT data. *Mon. Wea.*

Rev., **140**, 811–824, doi: 10.1175/MWR-D-10-05062.1.

Chan, K. T. F., and J. C. L. Chan, 2013: Angular momentum transports and synoptic flow patterns associated with tropical cyclone size change. *Mon. Wea. Rev.*, **141**, 3985–4007, doi: 10.1175/MWR-D-12-00204.1.

Chan, K. T. F., and J. C. L. Chan, 2014: Impacts of initial vortex size and planetary vorticity on tropical cyclone size. *Quart. J. Roy. Meteor. Soc.*, **140**, 2235–2248, doi: 10.1002/qj.2292.

Chan, K. T. F., and J. C. L. Chan, 2018: The outer-core wind structure of tropical cyclones. *J. Meteor. Soc. Japan*, **96**, 297–315, doi: 10.2151/jmsj.2018-042.

Chavas, D. R., N. Lin, and K. Emanuel, 2015: A model for the complete radial structure of the tropical cyclone wind field. Part I: Comparison with observed structure. *J. Atmos. Sci.*, **72**, 3647–3662, doi: 10.1175/JAS-D-15-0014.1.

Emanuel, K., 2005: Increasing destructiveness of tropical cyclones over the past 30 years. *Nature*, **436**, 686–688, doi: 10.1038/nature03906.

Emanuel, K. A., 1999: Thermodynamic control of hurricane intensity. *Nature*, **401**, 665–669, doi: 10.1038/44326.

Grinsted, A., J. C. Moore, and S. Jevrejeva, 2012: Homogeneous record of Atlantic hurricane surge threat since 1923. *Proc. Natl. Acad. Sci. USA*, **109**, 19,601–19,605, doi: 10.1073/pnas.1209542109.

Hack, J. J., and W. H. Schubert, 1986: Nonlinear response of atmospheric vortices to heating by organized cumulus convection. *J. Atmos. Sci.*, **43**, 1559–1573, doi: 10.1175/1520-0469(1986)043<1559:NROAVT>2.0.CO;2.

Henley, B. J., J. Gergis, D. J. Karoly, et al., 2015: A Tripole Index for the Interdecadal Pacific Oscillation. *Climate Dyn.*, **45**, 3077–3090, doi: 10.1007/s00382-015-2525-1.

Hill, K. A., and G. M. Lackmann, 2009: Influence of environmental humidity on tropical cyclone size. *Mon. Wea. Rev.*, **137**, 3294–3315, doi: 10.1175/2009MWR2679.1.

Kimball, S. K., and M. S. Mulekar, 2004: A 15-year climatology of North Atlantic tropical cyclones. Part I: Size parameters. *J. Climate*, **17**, 3555–3575, doi: 10.1175/1520-0442(2004)017<3555:AYCONA>2.0.CO;2.

Knaff, J. A., C. R. Sampson, M. DeMaria, et al., 2007: Statistical tropical cyclone wind radii prediction using climatology and persistence. *Wea. Forecasting*, **22**, 781–791, doi: 10.1175/WAF1026.1.

Kossin, J. P., 2019: Reply to: Moon, I.-J. et al.; Lanzante, J. R. *Nature*, **570**, E16–E22, doi: 10.1038/s41586-019-1224-1.

Kossin, J. P., K. A. Emanuel, and G. A. Vecchi, 2014: The poleward migration of the location of tropical cyclone maximum intensity. *Nature*, **509**, 349–352, doi: 10.1038/nature13278.

Kossin, J. P., K. A. Emanuel, and S. J. Camargo, 2016: Past and projected changes in western North Pacific tropical cyclone exposure. *J. Climate*, **29**, 5725–5739, doi: 10.1175/JCLI-D-16-0076.1.

Kruk, M. C., K. R. Knapp, and D. H. Levinson, 2010: A technique for combining global tropical cyclone best track data. *J. Atmos. Oceanic Technol.*, **27**, 680–692, doi: 10.1175/2009JTECHA1267.1.

Lu, X. Q., H. Yu, X. M. Yang, et al., 2017: Estimating tropical cyclone size in the Northwestern Pacific from geostationary satellite infrared images. *Remote Sens.*, **9**, 728, doi: 10.3390/rs9070728.

Maclay, K. S., M. DeMaria, and T. H. Vonder Haar, 2008: Tropical cyclone inner-core kinetic energy evolution. *Mon. Wea. Rev.*, **136**, 4882–4898, doi: 10.1175/2008MWR2268.1.

Mantua, N. J., S. R. Hare, Y. Zhang, et al., 1997: A Pacific interdecadal climate oscillation with impacts on salmon production. *Bull. Amer. Meteor. Soc.*, **78**, 1069–1080, doi: 10.1175/1520-0477(1997)078<1069:APICOW>2.0.CO;2.

Matyas, C. J., 2010: Associations between the size of hurricane rain fields at landfall and their surrounding environments. *Meteor. Atmos. Phys.*, **106**, 135–148, doi: 10.1007/s00703-009-0056-1.

Merrill, R. T., 1984: A comparison of large and small tropical cyclones. *Mon. Wea. Rev.*, **112**, 1408–1418, doi: 10.1175/1520-0493(1984)112<1408:ACOLAS>2.0.CO;2.

Moon, I.-J., S.-H. Kim, and J. C. L. Chan, 2019: Climate change and tropical cyclone trend. *Nature*, **570**, E3–E5, doi: 10.1038/s41586-019-1222-3.

Moyer, A. C., J. L. Evans, and M. Powell, 2007: Comparison of observed gale radius statistics. *Meteor. Atmos. Phys.*, **97**, 41–55, doi: 10.1007/s00703-006-0243-2.

Murakami, H., Y. Q. Wang, H. Yoshimura, et al., 2012: Future changes in tropical cyclone activity projected by the new high-resolution MRI-AGCM. *J. Climate*, **25**, 3237–3260, doi: 10.1175/JCLI-D-11-00415.1.

Quiring, S., A. Schumacher, C. Labosier, et al., 2011: Variations in mean annual tropical cyclone size in the Atlantic. *J. Geophys. Res. Atmos.*, **116**, D09114, doi: 10.1029/2010JD015011.

Rayner, N. A., D. E. Parker, E. B. Horton, et al., 2003: Global analyses of sea surface temperature, sea ice, and night marine air temperature since the late nineteenth century. *J. Geophys. Res. Atmos.*, **108**, 4407, doi: 10.1029/2002JD002670.

Schubert, W. H., and J. J. Hack, 1982: Inertial stability and tropical cyclone development. *J. Atmos. Sci.*, **39**, 1687–1697, doi: 10.1175/1520-0469(1982)039<1687:ISATCD>2.0.CO;2.

Smith, T. M., and R. W. Reynolds, 2003: Extended reconstruction of global sea surface temperatures based on COADS data (1854–1997). *J. Climate*, **16**, 1495–1510, doi: 10.1175/1520-0442(2003)016<1495:EROGSS>2.0.CO;2.

Stern, D. P., J. L. Vigh, D. S. Nolan, et al., 2015: Revisiting the relationship between eyewall contraction and intensification. *J. Atmos. Sci.*, **72**, 1283–1306, doi: 10.1175/JAS-D-14-0261.1.

Sun, Y., Z. Zhong, Y. Ha, et al., 2013: The dynamic and thermodynamic effects of relative and absolute sea surface temperature on tropical cyclone intensity. *Acta Meteor. Sinica*, **27**, 40–49, doi: 10.1007/s13351-013-0105-z.

Sun, Y., T. Li, Z. Zhong, et al., 2018: A recent reversal in the poleward shift of western North Pacific tropical cyclones. *Geophys. Res. Lett.*, **45**, 9944–9952, doi: 10.1029/2018GL079686.

Vecchi, G. A., and B. J. Soden, 2007: Effect of remote sea surface temperature change on tropical cyclone potential intensity. *Nature*, **450**, 1066–1070, doi: 10.1038/nature06423.

Wang, S., and R. Toumi, 2018: A historical analysis of the mature stage of tropical cyclones. *Int. J. Climatol.*, **38**, 2490–2505, doi: 10.1002/joc.5374.

Weatherford, C. L., and W. M. Gray, 1988a: Typhoon structure as revealed by aircraft reconnaissance. Part I: Data analysis and climatology. *Mon. Wea. Rev.*, **116**, 1032–1043, doi: 10.1175/1520-0493(1988)116<1032:TSARBA>2.0.CO;2.

Weatherford, C. L., and W. M. Gray, 1988b: Typhoon structure as revealed by aircraft reconnaissance. Part II: Structural variability. *Mon. Wea. Rev.*, **116**, 1044–1056, doi: 10.1175/1520-0493(1988)116<1044:TSARBA>2.0.CO;2.

Webster, P. J., G. J. Holland, J. A. Curry, et al., 2005: Changes in tropical cyclone number, duration, and intensity in a warming environment. *Science*, **309**, 1844–1846, doi: 10.1126/science.1116448.

Wu, L. Y., and X. T. Lei, 2014: Preliminary research on the relationships between the inner core size and outer size of tropical cyclones and their intensity. *J. Trop. Meteor.*, **20**, 308–313, doi: 10.16555/j.1006-8775.2014.04.002.

Wu, Q. Y., and Z. X. Ruan, 2021: Rapid contraction of the radius of maximum tangential wind and rapid intensification of a tropical cyclone. *J. Geophys. Res. Atmos.*, **126**, e2020JD033681, doi: 10.1029/2020JD033681.

Xu, J., and Y. Q. Wang, 2010a: Sensitivity of the simulated tropical cyclone inner-core size to the initial vortex size. *Mon. Wea. Rev.*, **138**, 4135–4157, doi: 10.1175/2010MWR3335.1.

Xu, J., and Y. Q. Wang, 2010b: Sensitivity of tropical cyclone inner-core size and intensity to the radial distribution of surface entropy flux. *J. Atmos. Sci.*, **67**, 1831–1852, doi: 10.1175/2010JAS3387.1.

Xu, J., and Y. Q. Wang, 2015: A statistical analysis on the dependence of tropical cyclone intensification rate on the storm intensity and size in the North Atlantic. *Wea. Forecasting*, **30**, 692–701, doi: 10.1175/WAF-D-14-00141.1.

Zhao, J. W., R. F. Zhan, Y. Q. Wang, et al., 2018: Contribution of the interdecadal Pacific oscillation to the recent abrupt decrease in tropical cyclone genesis frequency over the western North Pacific since 1998. *J. Climate*, **31**, 8211–8224, doi: 10.1175/JCLI-D-18-0202.1.

Tech & Copy Editor: Qi WANG